Diffusion property and functional connectivity of superior longitudinal fasciculus underpin human metacognition

Running title: white matter structural integrity and human metacognition

Yunxuan Zheng [1,3 §], Danni Wang [4 §], Qun Ye [1, 5], Futing Zou [1, 6], Jia Yin [7*], Yao Li [4*], Sze Chai Kwok [1, 2, 3 *]

1. Shanghai Key Laboratory of Brain Functional Genomics, Key Laboratory of Brain Functional Genomics Ministry of Education, School of Psychology and Cognitive Science, East China Normal University, Shanghai 200062, China

2. Shanghai Key Laboratory of Magnetic Resonance, East China Normal University, Shanghai 200062, China

3. NYU-ECNU Institute of Brain and Cognitive Science at NYU Shanghai, Shanghai 200062, China

4. Institute for Medical Imaging Technology, School of Biomedical Engineering, Shanghai Jiao Tong University, Shanghai 200030, China

5. Department of Psychology (Scarborough), University of Toronto, Toronto, ON M1C 1A4, Canada

6. Department of Psychology, University of Oregon, Eugene, OR, 97403, USA

7. Department of Neurosurgery, Tenth People's Hospital of Tongji University, Shanghai 200072, China

[§]Y. Zheng and D. Wang contributed equally as co-first authors.

Correspondence:
Sze Chai Kwok (sze-chai.kwok@st-hughs.oxon.org); Yao Li (yaoli@sjtu.edu.cn); Jia Yin (jianyiyin@hotmail.com)

Funding: This work was supported by the National Natural Science Foundation of China (Grant No. 81671201; 81871083) and Shanghai Jiao Tong University Scientific and Technological Innovation Funds (2019QYA12).

Conflict of Interest: The authors declare no competing financial interests.

Abstract:

Metacognition as the capacity of monitoring one's own cognition operates across domains. Here, we addressed whether metacognition in different cognitive domains rely on common or distinct neural substrates with diffusion tensor imaging (DTI) and inter-areal functional connectivity techniques. After acquiring DTI and resting-state fMRI data, we asked participants to perform a temporal-order memory judgement task and a perceptual discrimination task, followed by trial-specific confidence judgments. DTI analysis revealed that the structural integrity (fractional anisotropy) in the anterior portion of right superior longitudinal fasciculus (SLF) was associated with both perceptual and mnemonic metacognitive abilities. When the mnemonic metacognitive ability was disrupted by TMS, the mnemonic metacognition scores did not correlate with SLF structural integrity anymore, revealing the causal relevance of this tract in memory metacognition. Furthermore, taking the dorsolateral PFC and IPL (both of which are connected by SLF) as seeds, we found perceptual and mnemonic metacognitive abilities to be associated with functional connectivity between DLPFC and VLPFC, whereas mnemonic metacognitive ability was selectively associated with connectivity between IPL and precuneus. These results illustrate the importance of SLF and a distinct white-matter grey-matter circuitry that supports human metacognition.

Keywords: Metacognition, DTI, superior longitudinal fasciculus, functional connectivity, structural integrity

Introduction:

The capacity of reflecting on one's own cognitive process is known as metacognition (Flavell, 1979; Fleming and Dolan, 2012; Yeung and Summerfield, 2012). Metacognition has been considered as the most crucial function emerged during evolution (Hayes, 2016). Given its crucial functions, researchers have endeavored to understand how a metacognitive judgment is computed (Fleming and Daw, 2017; Kepecs et al., 2008; Zylberberg et al., 2016), how it is disrupted in psychiatric disorders (Hauser et al., 2017a; Rouault et al., 2018a), and how its accuracy can be improved (Carpenter et al., 2019). Metacognition is an umbrella term for the higher-level cognition about the lower-level cognition in various domains (e.g., perception and memory). As cognitive processes are implemented in the brain, an interesting and important question is whether the neural circuit supporting metacognition is the same or distinct across different cognitive domains.

A large body of fMRI work have increasingly demonstrated a nuanced picture for this domain-generality issue of metacognition. For example, the dorsolateral prefrontal cortex (DLPFC) might be involved in reading out the information of primary decision-making and using it for computing both perceptual and mnemonic metacognitive judgements (Chua and Ahmed, 2016; Fleming and Dolan, 2012; Kwok et al., 2019; Rounis et al., 2010). Morales et al. (2018) reported that the dorsal anterior cingulate cortex (dACC) was active during metacognitive evaluation in both memory and perception tasks but also found the activation patterns decoded from a perception task in the posterior medial frontal cortex and ventral medial prefrontal cortex could predict metacognitive judgements in a memory task. In contrast to these domain-general components, other evidence also indicates domain-specific mechanisms. For example, accurate perceptual metacognition is dependent on the accessibility of performance-monitoring

information coded in the dACC to the anterior PFC (Allen et al., 2017; Fleming et al., 2010, 2014; McCurdy et al., 2013), whereas accurate memorial metacognition is dependent on memory-mediated regions such as the medial PFC, mid/posterior cingulate cortex, inferior parietal lobule (IPL) and precuneus (Baird et al., 2013; Chua et al., 2006; McCurdy et al., 2013; Simons et al., 2010; Ye et al., 2018).

Although much progress has been made on how cortical networks supporting metacognition in different domains, less is known about how white matter pathways, through which inter-regional information communicates, contribute to these cognitive processes. Fleming et al. (2010) reported that metacognitive ability on perception domain is positively correlated with the diffusion anisotropy in the genu of corpus callosum (or the callosum forceps minor) which links the anterior PFC. To our knowledge, Baird et al. (2015) were the only group to date directly compared the white matter microstructure related to perceptual and mnemonic metacognitive ability. They found that accurate metacognitive evaluation on a perception task positively correlated with the diffusion anisotropy underlying the ACC, whereas accurate metacognitive evaluation on a memory task positively correlated with the diffusion anisotropy of the white matter underlying the IPL, indicating metacognition in different cognitive domains might rely on distinct neural resources. Nevertheless, Baird and colleagues did not control for the local task properties nor the metrics quantifying the perceptual and mnemonic metacognitive ability, which might bias the comparison across domains (Rouault et al., 2018b). They also did not characterize the diffusion property at specific, finely-defined locations along white matter tracts and their relationship with metacognitive abilities, so that the actual extent of how white matter tracts contributes to metacognition in each cognitive domain might be underestimated (Teubner-Rhodes et al., 2016).

Therefore, the present investigation sought to elucidate the neurobiological mechanisms underpinning metacognition across two different domains at the white-matter diffusion property level. We used a diffusion tensor imaging (DTI) tractography technique, named as automated fibre quantification (AFQ; Yeatman et al., 2012, 2014), to perform intra-tract analysis of tissue features along the neuronal fibre tracts. This method gives sensitive measures of the white matter structural integrity and allows us to examine its relationship with metacognitive ability in different domains. Given the known neural substrates of metacognition, we selected the following three white matter tracts: The bilateral superior longitudinal fasciculus (SLF), which links the domain-general DLFPC to the premotor and inferior parietal cortex (Hecht et al., 2015); The bilateral cingulum bundle, which connects the domain-general ACC to the posterior parietal regions (Heilbronner and Haber, 2014); and the callosum forceps minor (CFM), which connects the perceptual metacognition related regions such as the left and right anterior PFC (Park et al., 2008).

Based on the white matter tract results, in this study, we also further examined which brain regions send/receive information via the tracts to support metacognition through resting state functional connectivity MRI analysis (fc-MRI). The associated functional connectivity (FC) of the cortical area would provide insight into the related functional features across different cognitive domains. We hypothesized that the diffusion property of the SLF and CB would correlate with both mnemonic and perceptual metacognitive ability, while the diffusion property of CFM would exclusively correlate with the perceptual metacognition. We also predicted that the functional connectivity between regions within the posterior parietal cortex might exclusively predict mnemonic metacognitive ability (memory domain specific), while the functional connectivity between sub-regions in the prefrontal cortex support both mnemonic and perceptual metacognition (domain general). As a control test, we also disrupted

the mnemonic metacognition via TMS on the precuneus (a region sensitive to meta-memory but not to meta-perception), and used the post-TMS meta-cognition scores for a set of anatomical-cognitive correlational tests to verify the functional relevance of the white matter tracts on metacognition.

Methods:

Participants

18 university students (7 females, aged 19-24 years) from East China Normal University participated in this study. All participants had normal or corrected-to-normal vision, reported no history of psychiatric and neurological disease, and no other contraindications for MRI. All participants gave written informed consent, and were financially compensated after completing the experiment. Data from one participant was removed given the head motion during DTI scanning. The study was ethically approved by University Committee on Human Research Protection of East China Normal University.

Behavioural tasks, Stimuli and Analysis

The behavioural paradigm employed a two-way factorial design. Participants were asked to firstly play 14 chapters of a video game *Beyond: Two Souls* a day before the actual experiment as the memory encoding session, and then went through a stimulus-matched memory (temporal order judgment; TOJ) task and a perception (visual discrimination) task. Each task had two sessions, and prior to each session, participants received 20-min repetitive TMS that targeted at the precuneus or the vertex (as control site) in a counterbalanced order (Figure 1A-B). In each trial of the TOJ memory task (Figure 1C), participants were presented with two images from the 14 chapters of the video game they played, and were required to choose the one that occurred earlier. Images were presented for 5 s, followed by a 3-s confidence rating period

where participants needed to report their confidence in the TOJ judgement. There were four available confidence ratings (i.e., “Very Low”, “Low”, “High”, or “Very High”), and participants were encouraged to make use of the whole confidence scale. The perception task followed a similar procedure with the memory task. In each trial, the same set of subject-specific paired images used in the memory task were presented to participants. However, we manipulated resolution differences between the images, and asked participants to report which one was clearer (or blurrier) and their associated confidence level (Figure 1C).

There were 480 trials in total for each cognitive task (2 sessions × 4 blocks × 60 trials per block), and each task lasted around 45 min. A two-alternative forced choice (2-AFC) design was used for both the perception and memory task, and the experiment -related parameters (i.e., number of trials; dimension, position and sequence of the presented stimulus; time limits for responses; and the inter-trial intervals) were set identical in both tasks. All the visual stimuli were presented with E-prime software (Psychology Software Tools), and the presentation order of the paired images were counterbalanced throughout the experiment. Participants performed the memory task under an fMRI environment where visual stimuli were back-projected via a mirror system, and then were recalled back to undertake the perception task in a dimly illuminated room with a 17-inch CRT monitor.

Stimuli

Memory task: Participants played seven subject-specific chapters of an action-adventure video game a day before each memory session for memory encoding. These subject-specific videos were recorded and then the visual stimuli were extracted from the videos. In each session of the memory task, 240 pairs of images were extracted and paired up for the TOJ task. Perceptual task: The same pairs of the images were then also used for the perception task. We used Python

Imaging Library to reduce the resolution of one of the two images (i.e., resizing the image to change the pixel dimension). The smaller the difference in the resolution between the two images, the harder for participants to discriminate the clearer one. According to participants' performance in the memory task, we classified five difficulty (i.e., resolution difference) levels for the perceptual task. To match participants' performance across the two tasks, we used an *n*-down/1-up adaptive staircase procedure to adjust the image resolution online and converge on ~71% performance.

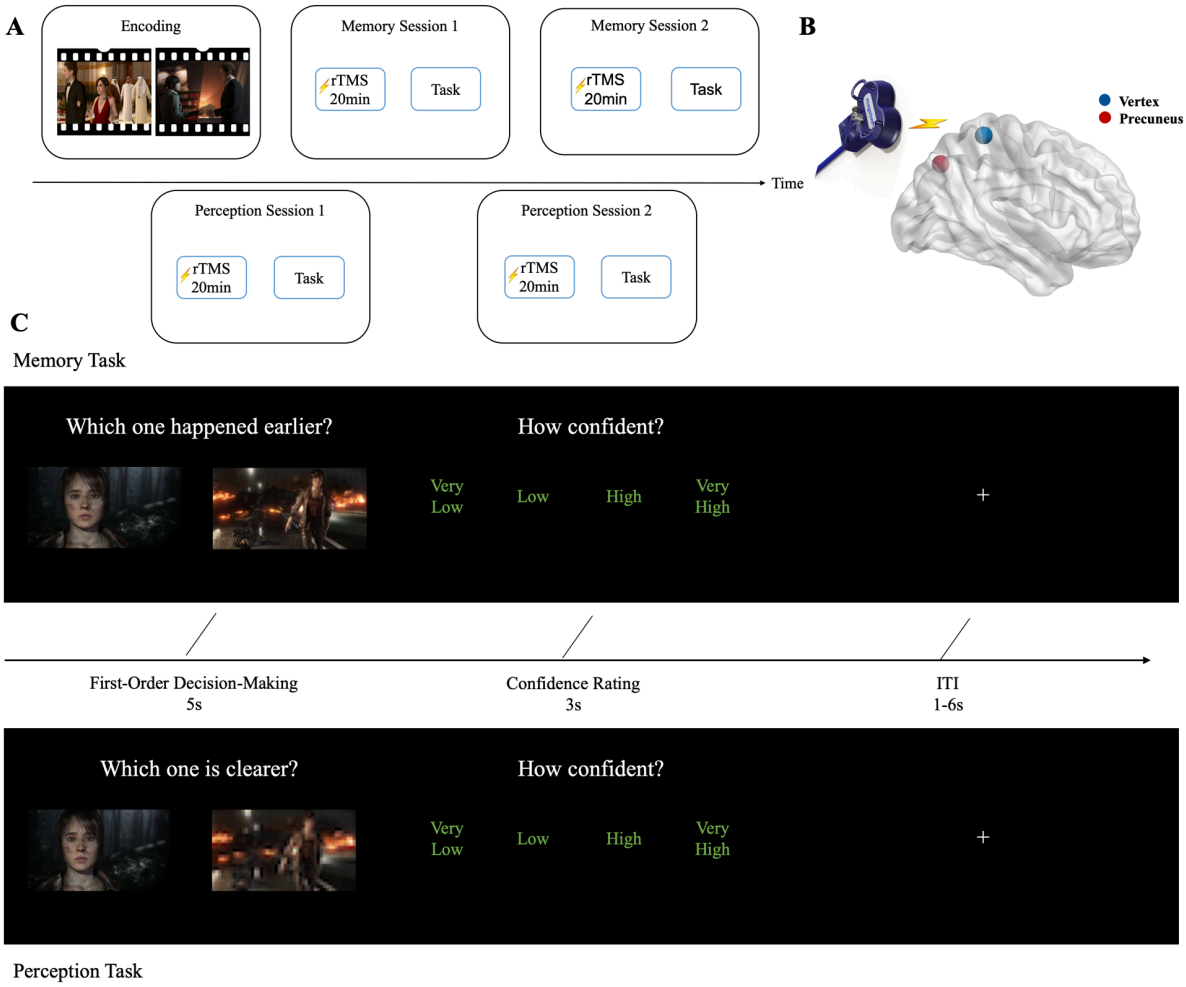

Figure 1. Study overview. ***A***, Experiment design. Prior to the main task in each session, participants received 20-min rTMS to one of the two cortical sites. ***B***, rTMS locations. The precuneus stimulation (MNI *x*, *y*, *z* = 6, -70, 44) was based on Kwok et al. (2012); vertex

stimulation as a control site. ***C***, Task Procedure. In the memory (temporal order judgement) task, participants were required to choose the image that occurred earlier in the video game; in the perceptual (visual discrimination) task, participants were required to identify which image was clearer (or blurrier). After each first-order decision making, participants rated their confidence per trial.

Behavioural analysis

Type-1 memory and perceptual performance were quantified d', a signal detection theoretic measure of type-I sensitivity. Type-2 metacognitive sensitivity was estimated by meta-d', which is expressed in the same scale as d' and indicates the extent to which a participant could discriminate correct responses from incorrect ones. Here we used metacognitive efficiency (meta-d' / d') to represent participants' metacognitive ability independent of primary decision-making performance. We quantified metacognitive ability through a hierarchical Bayesian Meta-d' model (Fleming, 2017). This computational model gives rise to more precise meta-d' estimation at both individual- and group-level (log-transformed) level, which allow direct comparison and correlation analyses of metacognitive abilities across conditions. Missed trials were discarded from the analysis (5.53%). RStudio and IBM SPSS 22 were used for the behavioural data analysis.

MR Image data acquisition

High- resolution structural, DTI, and resting-state fMRI data were acquired on a separate day prior to the first session. All MRI images were acquired using a 3.0 T Siemens Trio MRI scanner with a 32-channel head coil. High-resolution T1-weighted images were acquired using Magnetization Prepared Rapid Gradient Recalled Echo (MPRAGE) sequence with the following parameters: repetition time (TR) = 2530 ms, echo time (TE) = 2.34 ms, inversion

time = 1100 ms, flip angle = 7°, field of view (FOV) = 256 mm, slice number = 192, voxel size = 1 × 1 × 1 mm^3, slice thickness = 1.0 mm.

Seventy transverse DWI (diffusion-weighted imaging) slices were acquired with the parameters: TR = 11000 ms, TE = 98 ms, FOV = 256 mm, voxel size = 2 × 2 × 2 mm^3, acquisition matrix = 128 × 128, phase encoding direction: anterior to posterior (A > > P), 60 gradient directions (b = 1000 s/mm^2) and 2 non-diffusion images were obtained. The fMRI images were collected with the following parameters: TR = 2000 ms, TE = 30 ms, FOV = 230 mm, flip angle = 70°, voxel size = 3.6 × 3.6 × 4 mm^3, slice number = 33, parallel to the AC-PC plane. For each subject, 220 whole-brain volumes were acquired.

MR Image processing

Tract-based analysis for DTI data

For tract-based analysis, we performed DTI image preprocessing using VISTASOFT package (http://web.stanford.edu/group/vista/cgi-bin/wiki/index.php/Software). After the correction of head motion and eddy-current distortion, the DWI images were registered to the averaged non-diffusion weighted images. After that, the DWI images were registered to the T1-weighted image and the corresponding fractional anisotropy (FA). FA ranges from 0 to 1, and represents the direction of diffusion. The higher FA implies higher white matter structural integrity, thereby allowing stronger structural connectivity between the brain regions that are connected by the white matter (Greicius et al., 2009).

Fiber tracking was performed using Automating Fiber-Tract Quantification (AFQ, https://github.com/jyeatman/AFQ; Yeatman et al., 2012). First, a deterministic streamline tracking algorithm (Basser et al., 2000; Mori et al., 1999) was employed for whole-brain

tractography. The tracking is performed within the white matter mask, seeded at the voxels with FA > 0.3 and terminated if the voxel FA value is below 0.2 or the minimum angle between last path segment and next step direction is larger than 30° (Yeatman et al., 2012). Second, we performed fiber tract segmentation by a two way-point ROI procedure. The fiber is included in the fiber tract if it passes through two ROIs that define the trajectory of the fiber tract. The ROIs defined in Montreal Neurological Institute (MNI) space is registered to each participant's native space through nonlinearly transformation (Dougherty et al., 2005; Wakana et al., 2007). Finally, the candidate fiber is compared to the fiber tract probability map (Hua et al., 2008) and is further removed if it passes through white matter regions unlikely belonging to the fiber tract (Yeatman et al., 2012). The obtained tract is centered in all the corresponding tract fibers. A curve is created by defining 100 evenly spaced sample points along each fiber and calculating the mean position of each sample point in the curve accordingly. The fibers are removed if passing through the white matter regions unlikely the parts in fiber tract probability map or the three-dimensional Gaussian covariance of the sample points are larger than 5 s.d. from the mean. The diffusion metric, FA, was calculated as a weighted average of each individual fiber's measurement at each sample point. Five frontal-parietal white matter tracts (i.e., right/left superior longitudinal fasciculus, SLF; right/left cingulum bundle, CB; the callosum forceps minor, CFM) were selected for further analysis.

Functional connectivity analysis for fMRI data

For the functional connectivity (FC) calculation, the fMRI image processing was performed using Data Processing Assistant for Resting-State fMRI (DPARSF, https://www.nitrc.org/projects/dparsf/), which is based on Statistical Parametric Mapping 8 (SPM8, http://www.fil.ion.ucl.ac.uk/spm) and Resting-State fMRI Data Analysis Toolkit (REST v1.8, http://www.restfmri.net). The first 10 functional volumes were discarded for

machine stabilization and participants' adaption to the environment. The remaining 210 functional volumes were subsequently preprocessed by the following steps: including slice-timing, head motion correction, normalization to the MNI space with voxel size resampled to $3 \times 3 \times 3$ mm^3, spatial smoothing using an isotropic Gaussian filter kernel with 6 mm full-width at half maximum (FWHM), linear detrending, nuisance signal regression and temporal band-pass filtering (0.01-0.10 Hz). No participant was excluded if the head motion is above 3 mm or 3°. Nuisance regressors included Friston's 24 head motion parameters (Friston et al., 1996), white matter and CSF signals and global signal. The FC map was generated by computing the averaged time series in each seed ROI and correlating them with the time series of all other grey matter voxels in the whole brain using Pearson's correlation. The FC map was transformed to Z-score map by Fisher's Z transformation for statistical analysis.

Statistical analysis

To obtain significant FCs with the seed region, one-sample t-tests were performed for all the subjects. Statistical significance was set at $p < 0.05$ and a minimum cluster size of 223 voxels, with multiple comparison correction performed using AlphaSim program (M = 1000). The correlations between the cognitive scores and significant FCs were calculated using Pearson correlation analysis, with significance set at $p < 0.005$ and cluster size of 26 voxels, corrected for multiple comparison using AlphaSim (M = 1000). The correlations between DTI metrics and cognitive cores were calculated using Pearson correlation analysis with SPSS 20 (https://www.ibm.com/analytics/spss-statistics-software). The significance level was set at $p < 0.05$, controlled for multiple-comparisons error with false discovery rate (FDR) correction.

Repetitive TMS: procedure, protocol, and sites

In a related study, we diminished the mnemonic metacognitive efficiency with repetitive transcranial magnetic stimulation (rTMS) on the same participants. In the present study, in order to verify the functional relevance of white-matter tracts and their functional connectivity in support of metacognition, we made use of the TMS results here (but see our new analyses in Figure S1). The experimental details of rTMS were reported previously (Ye et al., 2018). In brief, rTMS was applied using a Magstim Rapid^2 magnetic stimulator connected to a 70 mm double air film coil (The Magstim Company, Ltd., Whitland, UK). To localize the target brain regions, Brainsight2.0 (Rogue Research Inc., Montreal, Canada) was used for the subject-specific structural T1-weighted images. Participants' brains were normalised by transforming to the Montreal Neurological Institute (MNI) template. To prepare the subject-image registration and promote online processing of the neuronavigation system, four location information of each subject's head were obtained manually by touching the tip of the nose, the nasion, and the inter-tragal notch of each ear using an infra- red pointer. In each session, rTMS was delivered to either the precuneus or vertex before the main task. TMS was applied at 1 Hz frequency for a continuous duration of 20 min (1200 pulses in total) at 110% of active motor threshold. The order of stimulation sites was counterbalanced across sessions. The coil was held to the scalp of the participant with a custom coil holder and the subject's head was propped a comfortable position. Coil orientation was parallel to the midline with the handle pointing downward. The stimulation sites are in the precuneus with MNI coordinates x = 6,y = -70, z= 44 (Kwok et al., 2012) and in a control area on the vertex (Jung et al., 2016); the latter is identified at the point of the same distance to the left and the right pre-auricular, and of the same distance to the nasion and the inion (Figure 1B).

Results

Behaviour

2 (cognitive domains) x 2 (TMS sites) repeated-measures ANOVA on d' revealed that participants performed better in perception tasks than in memory tasks (i.e., significant main effect of cognitive domains, $F(1,16) = 85.02$, $p<.001$), and TMS did not affect participants' primary decision-making. In terms of confidence rating, 2 (cognitive domains) x 2 (TMS sites) x 2 (trial correctness) repeated-measures ANOVA on confidence rating showed that participants were more confident in perception task (significant main effect of cognitive domain, $F(1,16)=7.094$, $p = .017$) and correct trials (significant main effect of trial correctness, $F(1,16) = 176.954$, $p <.001$), again without any TMS effect.

By fitting the Bayesian hierarchical meta-d' model, we observed however that, in comparison to the vertex TMS, the precuneus TMS significantly diminished the value of group-level metacognitive efficiency in memory task ($p_{\Delta\theta>0} \sim .95$; 95% HDI = [-.024, 0.406]), but not in perception task ($p_{\Delta\theta>0} \sim .31$; 95% HDI = [-.16, 0.10]). We also observed that the metacognitive efficiency for memory and perception tasks were significantly positively correlated in the vertex condition ($\rho=.517$, 95% HDI = [.003, .963]), which implies a domain-generality in metacognition (Figure S1).

DTI Results

For the DTI analysis, we used the fractional anisotropy (FA) value to represent white matter diffusion property. The AFQ method we used here tracks the superior longitudinal fasciculus (SLF) from the precentral gyrus to the inferior parietal lobe (IPL) (Figure 2A), the cingulum bundle (CB) portion that connects superior frontal gyrus, dorsal anterior cingulate cortex and precuneus (Figure S2A), and the whole the callosum forceps minor (CFM) that connects bilateral anterior prefrontal gyrus (Figure S2B).

First and foremost, we found significant positive correlations between the FA in the anterior portion of right SLF and memory metacognition (nodes 1-59, FA: R = [0.55, 0.77], p_{FDR} < 0.05) as well as with perceptual metacognition (nodes 1-42, FA: R = [0.58, 0.71], p_{FDR} < 0.05) in the TMS-vertex condition (Figure 2B-C, top panel). Notably, when TMS was applied to the precuneus, only the correlation between right SLF FA and perceptual metacognition survived (nodes 7-43, FA: R = [0.47, 0.70], p_{FDR} < 0.05, Figure 2B-C, bottom panel). This is confirmed by a 2-way repeated-measures ANOVA that there is a significant interaction between cognitive domains and TMS (precuneus or vertex) modulation in the correlation coefficients along SLF nodes ($F(1,58) = 516.726$, $p<.001$). Post-hoc t-tests confirm that TMS to the precuneus significantly reduces the correlation in the memory domain ($t(58)=30.545$, $p<.001$) but not in the perception domain ($t(58)=1.453$, $p=.152$) (cf. behavioural results in Figure S1A).

The metacognitive index is based on how people rate their confidence, which refer to how meaningful a person's confidence rating is in distinguishing between correct and incorrect responses. We accordingly looked into how SLF-metacognition correlations might manifest differently for correct vs. incorrect responses. Indeed, the correlation between FA (nodes 1-59) and confidence rating were affected by TMS differentially for correct trials and incorrect trials in memory task (interaction effect, $F(1,58)=381.67$, $p<.001$). TMS on the precuneus only reduced the correlation coefficients for correct trials ($t(58)=-27.224$, $p <.001$) but not for incorrect trials ($t(58)=-.504$, $p=.616$). Additionally, we did not find any significant node along SLF that correlate with subjects' primary decision accuracy, or overall mean confidence rating level in both cognitive tasks. These indicate that the reported effects regarding the SLF tract are specific to metacognitive efficiency rather than with primary decision-making performances.

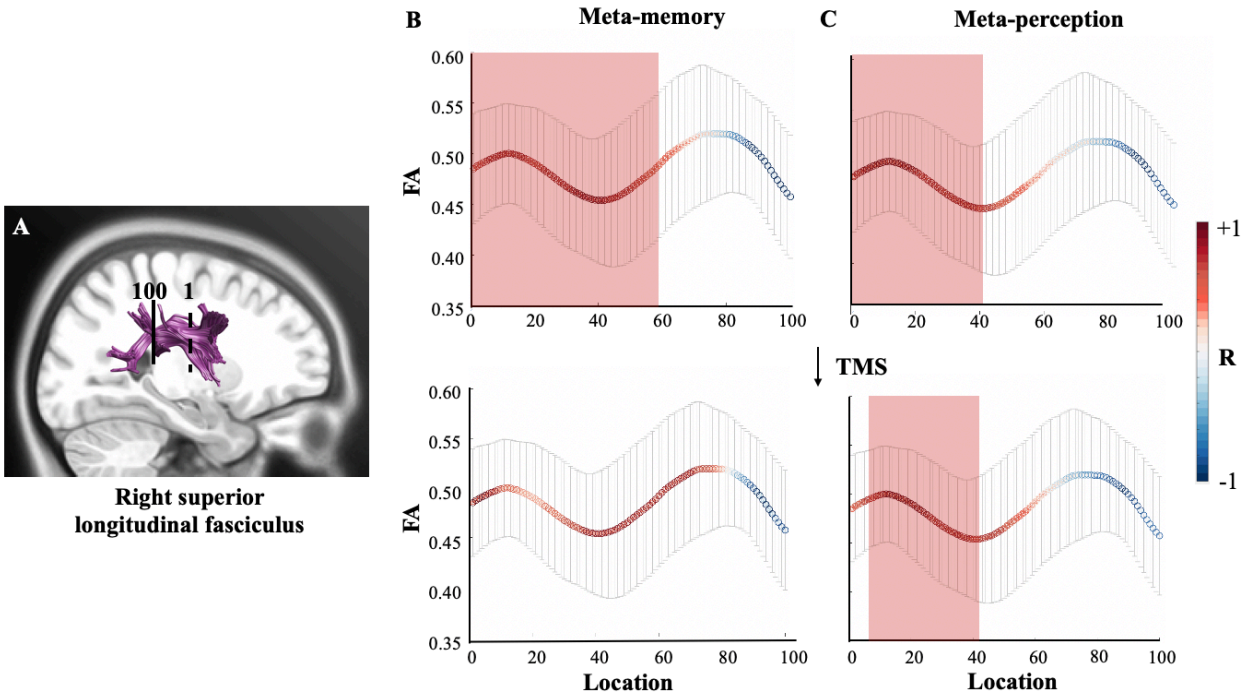

Figure 2. DTI results. The FA of the nodes along the right SLF had positive correlations with both perceptual and mnemonic metacognitive efficiency. ***A***, the portion of SLF that was tracked and evenly divided into 100 nodes by the AFQ method. The dash line represents the location of the starting point (marked by numeral 1) and the solid line represents the location of the ending point (marked by numeral 100). ***B*** and ***C*** respectively illustrates the correlation between the FA value of each SLF node and mnemonic or perceptual metacognitive efficiency (Top two panels: without TMS to precuneus; bottom two panels: TMS to precuneus). Notably, TMS to the precuneus eliminated the correlation between right SLF FA and memory metacognition scores. The x-axis is the individual node alongside the SLF, and its corresponding FA value is shown on y-axis. The colour of the curved lines illustrates the correlation between the FA of a SLF node and metacognitive efficiency scores. Those nodes that had significant correlation with metacognitive efficiency scores are marked by a red rectangular. The error bars denote standard error of the means over participants. Notes: DTI, diffusion tensor imaging; FA, fractional anisotropy; AFQ, Automating Fiber-Tract Quantification; SLF, superior longitudinal fasciculus; TMS, transcranial magnetic stimulation.

Moreover, we observed that the FA of the callosum forceps minor, which connects to the bilateral aPFC, exhibit positive correlations with mnemonic metacognition (nodes 8-14, 19-25, 66-74, 91-95, FA: R = [0.51, 0.66], $p_{unc} < 0.05$) and with perceptual metacognition (9-14, 41-42, 44-47, 65-75, FA: R = [0.50, 0.64], $p_{unc} < 0.05$) albeit at an uncorrected threshold. Similarly, the FA of the cingulum bundle portion, which extends to the dACC, also had positive correlations with both mnemonic and perceptual metacognitive ability (Mnemonic: nodes 26-34, 85-93, FA: R = [0.50, 0.62], $p_{unc} < 0.05$; Perceptual: nodes 26-32, FA: R = [0.55, 0.69], $p_{unc} < 0.05$) at an uncorrected threshold (Figure S2).

Functional connectivity MRI (fc-MRI) Results

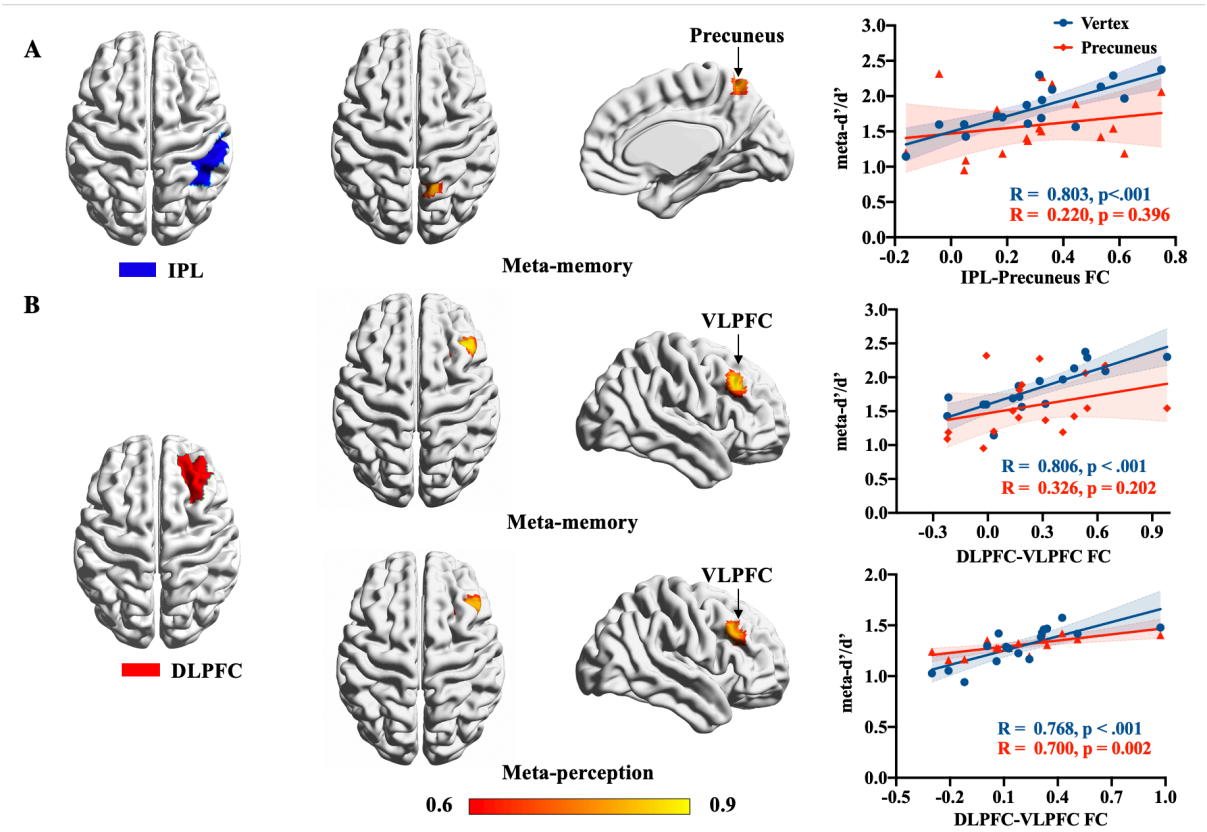

Figure 3. Functional connectivity results. ***A***. With the right IPL (A40rd in BA atlas) selected as seed, the IPL – Precuneus FC selectively correlated with mnemonic metacognitive

efficiency in the TMS-vertex condition. ***B***. With the right DLPFC (A9/46d in BA atlas) selected as seed, the DLPFC – VLPFC FC correlated with both perceptual and mnemonic metacognitive efficiency in TMS-vertex condition. When TMS was applied at the precuneus, the correlation with mnemonic metacognition diminished. Notes: fMRI, functional magnetic resonance imaging; IPL, inferior parietal lobe; FC, functional connectivity; TMS, transcranial magnetic stimulation; DLPFC, dorsolateral prefrontal cortex; VLPFC, ventrolateral prefrontal cortex; BA, Brainnetome Atlas.

Based on the white matter tract results, we then examined which brain regions send/receive information via the SLF to support metacognition in each domain through rs-fcMRI analysis. As the right SLF anatomically connects the right IPL and right DLPFC, we selected these two cortical regions as the seeds for the rs-fcMRI analysis (right IPL: A40rd in BA atlas, which is directly touched by the tracked SLF, Figure 3A; right DLPFC: A9/46d in BA atlas, Figure 3B). As illustrated in Figure 3A, the significant correlation between the activity of right IPL and right precuneus was differentially correlated with the mnemonic metacognitive efficiency under TMS vertex condition (precuneus: peak voxel MNI location, [15, -60, 63], Figure 3A middle panel). This correlation was however significantly reduced in the data following TMS on the precuneus (comparison between correlations: z = 2.34, p = .019).

For the right DLPFC seed, we observed that the significant resting-state FC between the right DLPFC and ventrolateral PFC (VLPFC) significantly correlated with both perceptual and mnemonic metacognitive efficiency under the control TMS condition (VLPFC: peak voxel MNI location, [45, 24, 36] and [42, 27 36] for perception and memory respectively, Figure 3B middle panel). However, as depicted in Figure 3B right panel, with TMS on the precuneus, the correlation between DLPFC–VLPFC FC and mnemonic metacognitive efficiency was

significantly reduced (comparison between correlations: z = 2.06, p = .039), whereas the correlation with perceptual metacognitive efficiency remained unchanged (comparison between correlations: z = .39, p = .696).

Discussion:

Whether the computation of metacognition relies on the same mechanism across cognitive domains has been a controversial issue. In the present study, we addressed this domain-generality/specificity issue at the white matter structural integrity and grey matter functional connectivity level. By using DTI and resting-state fMRI techniques, we found both domain-general and domain-specific components supporting the metacognitive performance in perception and memory tasks.

We observed that the right SLF serves a domain-general role in connection on metacognition. The structural integrity of the anterior portion of this tract correlates significantly with metacognitive efficiency in both perception and memory tasks, but not with primary decision-making performance nor confidence rating level. This specific portion of the right SLF underlies the precentral gyrus and links the right DLPFC to the right IPL (Hecht et al., 2015). Additionally, it also lies within the frontal lobe, which is not mixed by the temporal fibres in the Arcuate Fasciculus (Wakana, 2007) and is indicative of the DLPFC – IPL communication (Yeatman et al., 2012). On one end, the right DLPFC is involved in both perceptual and mnemonic metacognition in both humans and monkeys, and suggested as reading out information related to primary decision-making and computing metacognitive judgements (Fleming and Dolan, 2012; Kwok et al., 2019; Morales et al., 2018; Shekhar and Rahnev, 2018). On the other end, the right IPL has been identified as crucial in mnemonic metacognition

(Berryhil et al., 2007; Davidson et al., 2008; Simons et al., 2010). Moreover, the right IPL has also been reported as the "output gating" of working memory for information selection (Baddeley, 2000; Vilberg and Rugg, 2008; Wallis et al., 2015). Thus, given the functional meaning of white-matter structural integrity, we propose that, in a metacognitive process, the right IPL select what information regarding the previous decision-making should be used and convey it to the right DLPFC through SLF for further computation. The better structural integrity of the right SLF is, the lower noise will be added during the information transmission, allowing the right DLPFC to read out more precise information for the metacognitive computation.

Several studies recently found that the premotor and/or motor areas could carry action information of primary decision-making (i.e., response fluency and competition) or reflect the cognitive states to guide metacognitive evaluation (de Lange et al., 2013; Fleming et al., 2015; Susser and Mulligan, 2015; Wokke et al., 2020). As the precentral gyrus, the region directly connected by the targeted portion of SLF, encompasses the dorsal premotor cortex and primary motor cortex (Schubotz et al., 2010), perhaps the SLF might subserve the transmission of such action information to support metacognition irrespective of domains. However, if this is the case, then the TMS on the precuneus should either disrupt the use of action information in both cognitive tasks or result in no disruption at all, and in turn produce either a general effect or no effect on the SLF FA – metacognition correlation. Given the precuneus TMS selectively shifts the SLF FA – metacognition correlation in the memory domain, we therefore reject this alternative explanation.

We next examined how the intrinsic functional connectivity of the right IPL and right DLPFC contributes to metacognition in each domain. We found that the stronger functional connection

between the right DLPFC and right VLPFC is, the better an agent can discriminate correct responses from incorrect ones irrespective of cognitive domains. Shekhar and Rahnev (2018) suggested the other prefrontal regions such as aPFC might receive the information from the DLPFC to compute the metacognitive evaluation. Perhaps, the right VLPFC is also involved in the metacognition computation process (Wu et al., 2015). Alternatively, the right VLPFC might help select the rating responding to the metacognitive evaluation from the right DLPFC (Levy and Wagner, 2012).

In contrast to domain-general DLPFC – VLPFC connectivity, the functional connectivity between right IPL and precuneus exclusively correlates with mnemonic metacognitive ability, suggesting that the presence of two different sets of components supporting the conscious monitoring on each specific cognitive process. The precuneus has been linked to generating mental images to aid detailed episodic memory retrieval (Fletcher et al., 1995; Hebscher et al., 2020; Koch et al., 2018; Richter et al., 2016; Sreekumar et al., 2018). Our finding on the relationship between the right IPL – precuneus connectivity and mnemonic metacognitive ability lends support to the hypothesis that mnemonic metacognition relies on the read out of memory trace (Nelson and Narens, 1990). Notably, when TMS was applied on the precuneus, the relationship between one's SLF structural integrity and their confidence rating's efficiency in distinguishing between correct and incorrect responses was eradicated in the memory task (but not in the perceptual task). This suggests that the IPL – DLPFC network makes use of the memory information from the precuneus for metacognitive decisions. Together with the precuneus - hippocampus connectivity (Ye et al., 2019), a cortico-hippocampal network of meta-mnemonic process is at work with primary mnemonic processes (McClelland et al., 1995; Wang et al., 2014; Zeidman et al., 2015), implicating the hippocampus in initiating the retrieval

of the memory traces, which are then integrated to detailed recollections and conscious monitoring supported by the precuneus and the IPL (Richter et al., 2016).

Arguably, the results of current study could support the hierarchical model of metacognition. The hierarchical model proposes that metacognition and primary decision-making are two distinct cognitive processes: the primary decision-making is implemented at a first order, while a metacognitive process access both sensory evidence for the decision-making and other sources of information to form a judgement (Fleming & Daw, 2017). Many studies have reported such dissociation between metacognition and decision-making, with the PFC playing a central role in the hierarchical monitoring (Allen et al., 2017; Bang et al., 2019; Fleming et al., 2014; Hauser et al., 2017b; Qiu et al., 2018; Rounis et al., 2010; Shekhar and Rahnev, 2018). If metacognition relies on a hierarchical architecture, it is reasonable to assume that the hierarchical monitoring to be domain-general. Indeed, the structural integrity of the right SLF correlates with both perceptual and mnemonic metacognitive performance here, but this microstructural feature was not relevant to the first-order decision-making performance (such as confidence rating). Moreover, albeit at an uncorrected threshold, corroborating with Fleming and colleagues (2010), we found that the structural integrity of the cingulum bundle (CB) and the callosum forceps minor (CFM) have domain-general associations with metacognition. The CB extends to the dACC, whereas the CFM is connected to the bilateral aPFC. This suggests a white-matter grey-matter circuitry linking the dorsal anterior –posterior parietal– prefrontal regions might be at play in a hierarchical order to support the multi-way information input-output flow underlying effective mnemonic metacognition.

On a more speculative note, metacognition has been associated with states of consciousness (Rosenthal, 2019), and our current result might help facilitate the understanding on the

neurocognitive mechanisms underlying consciousness. Several studies have revealed that subjective conscious awareness is dissociated from the objective visual perception, and requires the involvement of the prefrontal and parietal cortices apart from primary sensory regions (Bartolomeo et al., 2007; Colas et al., 2019; Del Cul et al., 2009; Lau and Passingham, 2006). It has also been argued that to generate conscious experiences, a higher-level neural circuit needs to metacognitively access the primary sensory representation from the lower-level neural circuit to the working memory (Dehanene and Changeux, 2011; Lau and Rosenthal, 2011; Shea and Frith, 2019). Indeed, our results imply that, to form a conscious metacognitive evaluation, the IPL firstly represents first-order decision-making related information in the memory and then conveys it to the DLPFC via the SLF for further monitoring. Incidentally, in the patients with right DLPFC lesion the structural integrity of the right SLF was significantly correlated with their subjective visual conscious experiences but not objective perception task performance (Colás et al., 2019). Moreover, the white-matter volume of the right SLF also predicts the metacognitive beliefs of schizophrenia patients (Spalletta et al. 2014). These clinical findings are in line with ours in the health, thereby reinforcing the possibility that the SLF is indeed needed for the higher-level conscious assessment of mental processes.

There are several caveats to consider. First, the current study only concerns the two broad cognitive domains of perception and memory. Future research could test whether our "domain-general" results are applicable to other cognitive domains. Second, further research could employ the diffusion spectrum imaging (DSI) technique to examine the crossing fibres across voxels to elucidate the structural integrity of the posterior portion of the SLF. Since the functional connectivity we measured here was at resting states, and it reflects only stable individual differences (e.g., cognitive skills and/or personality traits) which might be dissociable from activations during task-states (Hampson et al., 2006; Seeley et al., 2007).

Future research could also consider using task-state fMRI together with dynamic casual modelling (Friston, 2011) to draw a more comprehensive picture of the neural circuit of metacognition.

In conclusion, this investigation reveals how perceptual and mnemonic metacognition is supported by the structural integrity of the SLF and its functional connectivity with connecting brain regions. The right SLF, which connects the right IPL and right DLPFC, substantiates a domain-general informational pathway for perceptual and mnemonic metacognition. Based on the rs-fcMRI results, the right VLPFC might assist the right DLPFC in computing metacognitive evaluations across cognitive domains, whereas the right IPL access memory information from the precuneus and convey such information to the right DLPFC for mnemonic metacognitive computation. Together with the cingulum bundle and the callosum forceps minor, a complex white-matter grey-matter circuitry linking the dorsal anterior cingulate – posterior parietal –prefrontal regions might be at play to support the information flow underlying effective metacognitive mechanisms and ultimately our state of consciousness.

References:

Allen M, Glen JC, Müllensiefen D, Schwarzkopf DS, Fardo F, Frank D, Callaghan MF, Rees G. 2017. Metacognitive ability correlates with hippocampal and prefrontal microstructure. *Neuroimage*. 149:415-423.

Baddeley, A. 2000. The episodic buffer: a new component of working memory?. *Trends Cogn Sci*. 4(11): 417-423.

Baird B, Cieslak M, Smallwood J, Grafton ST, Schooler JW. 2015. Regional white matter variation associated with domain-specific metacognitive accuracy. *J Cogn Neurosci*. 27(3). 440-452.

Baird B, Smallwood J, Gorgolewski KJ, Margulies DS. 2013. Medial and lateral networks in anterior prefrontal cortex support metacognitive ability for memory and perception. *J Neurosci*. 33(42): 16657-16665.

Bang J, Shekhar M, Rahnev D. 2019. Sensory Noise Increases Metacognitive Efficiency. *J Exp Psychol Gen* 148(3): 437-452.

Bartolomeo P, Decaix C, Siéroff E. 2007. The phenomenology of endogenous orienting. *Conscious Cogn*. 16(1): 144-161.

Basser PJ, Pajevic S, Pierpaoli C, Duda J, Aldroubi A. 2000. In vivo fiber tractography using DT-MRI data. *Magn Reson Med*. 44: 625– 632.

Berryhill ME, Phuong L, Picasso L, Cabeza R, Olson IR. 2007. Parietal lobe and episodic memory: bilateral damage causes impaired free recall of autobiographical memory. *J Neurosci*, 27:14415–14423.

Carpenter J., Sherman MT, Kievit RA, Seth AK, Lau H, Fleming SM. 2019. Domain-general enhancements of metacognitive ability through adaptive training. *J Exp Psychol Gen* 148(1): 51-64.

Chua EF, Ahmed R. 2016. Electrical stimulation of the dorsolateral prefrontal cortex improves memory monitoring. *Neuropsychologia*. 85: 74-79.

Colás I, Chica AB, Ródenas E, Busquier H, Olivares G, Triviño M. 2019. Conscious perception in patients with prefrontal damage. *Neuropsychologia*. 129: 284-293.

Davidson PS, Anaki D, Ciaramelli E, Cohn M, Kim AS, Murphy K J, Troyer AK, Moscovitch M, Levine B. 2008. Does lateral parietal cortex support episodic memory?: Evidence from focal lesion patients. *Neuropsychologia*. 46(7): 1743-1755.

de Lange FP, Rahnev DA, Donner TH, Lau H. 2013. Prestimulus oscillatory activity over motor cortex reflects perceptual expectations. *J Neurosci.* 33(4):1400-1410.

Dehaene S, Changeux JP. 2011. Experimental and theoretical approaches to conscious processing. *Neuron*. 70(2): 200-227.

Del Cul A, Dehaene S, Reyes P, Bravo E, Slachevsky A. 2009. Causal role of prefrontal cortex in the threshold for access to consciousness. *Brain*. 132(9): 2531-2540.

Dougherty RF, Ben-Shachar M, Deutsch GK, Hernandez A, Fox GR, Wandell BA. 2007. Temporal-callosal pathway diffusivity predicts phonological skills in children. *Proc Natl Acad Sci U S A*. 104(20): 8556-8561.

Flavell J. 1979. Metacognition and cognitive monitoring: A new area of cognitive-developmental inquiry. *Am Psychol*. 34(10): 906-911.

Fleming SM, Daw ND. 2017. Self-evaluation of decision-making: A general Bayesian framework for metacognitive computation. *Psychol Rev*. 124(1): 91-114.

Fleming SM, Dolan RJ. 2012. The neural basis of metacognitive ability. *Philos Trans R Soc Lond B Biol Sci*. 367(1594): 1338-1349.

Fleming SM, Maniscalco B, Ko Y, Amendi N, Ro T, Lau H. 2015. Action-specific disruption of perceptual confidence. *Psychol Sci*. 26(1):89-98.

Fleming SM, Ryu J, Golfinos JG, Blackmon KE. 2014. Domain-specific impairment in metacognitive accuracy following anterior prefrontal lesions. *Brain.* 137 (10): 2811-2822

Fleming SM, Weil RS, Nagy Z, Dolan RJ, Rees G. 2010. Relating introspective accuracy to individual differences in brain structure. *Science*. 329(5998): 1541-1543.

Fleming SM. 2017. HMeta-d: hierarchical Bayesian estimation of metacognitive efficiency from confidence ratings. *Neurosci Conscious*. 2017(1): nix007

Friston KJ, Williams S, Howard R, Frackowiak RS, Turner R. 1996. Movement-related effects in fMRI time-series. *Magn Reson Med*. 35(3):346-55.

Greicius MD, Supekar K, Menon V, Dougherty RF. 2009. Resting-state functional connectivity reflects structural connectivity in the default mode network. *Cereb Cortex*. 19(1): 72-78.

Hampson M, Driesen NR, Skudlarski P, Gore JC, Constable RT. 2006. Brain connectivity related to working memory performance. *J Neurosci*. 26(51): 13338-13343.

Hauser TU, Allen M, NSPN Consortium, Rees G, Dolan RJ. 2017a. Metacognitive impairments extend perceptual decision making weaknesses in compulsivity. *Sci Rep*. 7(1):1-10.

Hauser TU, Allen M, Purg N, Moutoussis M, Rees G, Dolan, RJ. 2017b. Noradrenaline blockade specifically enhances metacognitive performance. *Elife*. 6: e24901.

Hebscher M, Ibrahim C, Gilboa A. 2020. Precuneus stimulation alters the neural dynamics of autobiographical memory retrieval. *Neuroimage*. 116575.

Hecht EE, Gutman DA, Bradley BA, Preuss TM, Stout D. 2015. Virtual dissection and comparative connectivity of the superior longitudinal fasciculus in chimpanzees and humans. *Neuroimage*. 108: 124-137.

Heilbronner SR, Haber SN. 2014. Frontal cortical and subcortical projections provide a basis for segmenting the cingulum bundle: implications for neuroimaging and psychiatric disorders. *J Neurosci*. 34(30): 10041-10054.

Heyes C. 2016. Who knows? Metacognitive social learning strategies. *Trends Cogn Sci*. 20(3): 204-213.

Hua K, Zhang J, Wakana S, Jiang H, Li X, Reich DS, Calabresi PA, Pekar JJ, van Zijl PC, Mori S. 2008. Tract probability maps in stereotaxic spaces: analyses of white matter anatomy and tract-specific quantification. *Neuroimage*. 39(1): 336-47.

Jung J, Bungert A, Bowtell R, Jackson SR. 2016. Vertex stimulation as a control site for transcranial magnetic stimulation: a concurrent TMS/fMRI study. *Brain Stimulation*. 9(1): 58-64.

Kepecs A, Uchida N, Zariwala HA, Mainen ZF. 2008. Neural correlates, computation and behavioural impact of decision confidence. *Nature*. 455(7210): 227-231.

Koch G, Bonnì S, Pellicciari MC, Casula EP, Mancini M, Esposito R, Ponzo V, Picazio S, Di Lorenzo F, Serra L et al. 2018. Transcranial magnetic stimulation of the precuneus enhances memory and neural activity in prodromal Alzheimer's disease. *Neuroimage*. 169: 302-311.

Kwok SC, Cai Y, Buckley MJ. 2019. Mnemonic introspection in macaques is dependent on superior dorsolateral prefrontal cortex but not orbitofrontal cortex. *J Neurosci*. 39(30): 5922-5934.

Kwok SC, Shallice T, Macaluso E. 2012. Functional anatomy of temporal organisation and domain-specificity of episodic memory retrieval. *Neuropsychologia*. 50(12): 2943-2955.

Lau H, Rosenthal D. (2011). Empirical support for higher-order theories of conscious awareness. *Trends Cogn Sci*. 15(8): 365-373.

Lau HC, Passingham RE. 2006. Relative blindsight in normal observers and the neural correlate of visual consciousness. *Proc Natl Acad Sci U S A*. 103(49): 18763-18768.

Levy BJ, Wagner AD. 2011. Cognitive control and right ventrolateral prefrontal cortex: reflexive reorienting, motor inhibition, and action updating. *Ann N Y Acad Sci*. 1224(1): 40-62.

McClelland JL, McNaughton BL, O'Reilly RC. 1995. Why there are complementary learning systems in the hippocampus and neocortex: insights from the successes and failures of connectionist models of learning and memory. *Psychol Rev*. 102: 419–457

McCurdy LY, Maniscalco B, Metcalfe J, Liu KY, De Lange FP, Lau, H. 2013. Anatomical coupling between distinct metacognitive systems for memory and visual perception. *J Neurosci*. *33*(5): 1897-1906.

Morales J, Lau H, Fleming SM. 2018. Domain-general and domain-specific patterns of activity support metacognition in human prefrontal cortex. *J Neurosci*. 38(14): 3534-3546

Mori S, Crain BJ, Chacko VP, van Zijl PC. 1999. Three-dimensional tracking of axonal projections in the brain by magnetic resonance imaging. *Ann Neurol*. 45: 265–269.

Nelson TO, Narens L. 1990. Metamemory: A theoretical framework and new findings. *Psychol Learn Motiv*. 26: 125-141.

Park HJ, Kim JJ, Lee SK, Seok JH, Chun J, Kim DI, & Lee JD. 2008. Corpus callosal connection mapping using cortical gray matter parcellation and DT-MRI. *Hum Brain Mapp*. 29(5): 503-516.

Qiu L, Su J, Ni Y, Bai Y, Zhang X, Li X, Wan X. 2018. The neural system of metacognition accompanying decision-making in the prefrontal cortex. *PLoS Biol*, 16(4): e2004037.

Richter FR, Cooper RA, Bays PM, Simons JS. 2016. Distinct neural mechanisms underlie the success, precision, and vividness of episodic memory. *Elife*. 5: e18260.

Rosenthal D. (2019). Consciousness and confidence. *Neuropsychologia*. 128: 255-265.

Rouault M, Seow T, Gillan CM, Fleming SM. 2018a. Psychiatric symptom dimensions are associated with dissociable shifts in metacognition but not task performance. *Biol Psychiatry.* 84(6): 443-451.

Rouault M, McWilliams A, Allen MG, Fleming SM. 2018b. Human metacognition across domains: insights from individual differences and neuroimaging. *Personal Neurosci*, 1.

Rounis E, Maniscalco B, Rothwell JC, Passingham RE, Lau H. 2010. Theta-burst transcranial magnetic stimulation to the prefrontal cortex impairs metacognitive visual awareness. *Cogn Neurosci*. 1(3), 165-175.

Schubotz RI, Anwander A, Knösche TR, von Cramon DY, Tittgemeyer M. 2010. Anatomical and functional parcellation of the human lateral premotor cortex. *Neuroimage*. 50(2): 396-408.

Seeley WW, Menon V, Schatzberg AF, Keller J, Glover GH, Kenna H, Reiss AL, Greicius MD. 2007. Dissociable intrinsic connectivity networks for salience processing and executive control. *J Neurosci*. 27(9): 2349-2356.

Shea N, Frith CD. 2019. The Global Workspace Needs Metacognition. *Trends Cogn Sci*, 23(7), 560-571.

Shekhar M, Rahnev D. 2018. Distinguishing the roles of dorsolateral and anterior PFC in visual metacognition. *J Neurosci*. 38(22): 5078-5087.

Simons JS, Peers PV, Mazuz YS, Berryhill ME, Olson IR. 2010. Dissociation between memory accuracy and memory confidence following bilateral parietal lesions. *Cereb Cortex*. 20(2): 479-485.

Spalletta G, Piras F, Piras F, Caltagirone C, Orfei MD. 2014. The structural neuroanatomy of metacognitive insight in schizophrenia and its psychopathological and neuropsychological correlates. *Hum Brain Mapp*. 35(9): 4729-4740.

Susser JA, Mulligan NW. 2015. The effect of motoric fluency on metamemory. *Psychon Bull Rev*. 22(4):1014-1019.

Teubner-Rhodes S, Vaden KI, Cute SL, Yeatman JD, Dougherty RF, Eckert MA. 2016. Aging-resilient associations between the arcuate fasciculus and vocabulary knowledge: Microstructure or morphology?. *J Neurosci*. 36(27): 7210-7222.

Vilberg KL, Rugg MD. 2008. Memory retrieval and the parietal cortex: a review of evidence from a dual-process perspective. *Neuropsychologia*. 46:1787–1799.

Wakana S, Caprihan A, Panzenboeck MM, Fallon JH, Perry M, Gollub RL, Hua K, Zhang J, Jiang H, Dubey P et al. 2007. Reproducibility of quantitative tractography methods applied to cerebral white matter. *Neuroimage*. 36(3): 630-644.

Wallis G, Stokes M, Cousijn H, Woolrich M, Nobre AC. 2015. Frontoparietal and cingulo-opercular networks play dissociable roles in control of working memory. *J Cogn Neurosci*. 27(10): 2019-2034.

Wang JX, Rogers LM, Gross EZ, Ryals AJ, Dokucu ME, Brandstatt KL, Hermiller MS, Voss JL. 2014. Targeted enhancement of cortical-hippocampal brain networks and associative memory. *Science*. 345:1054–1057.

Wokke ME, Achoui D, Cleeremans A. 2020. Action information contributes to metacognitive decision-making. *Sci Rep*. 10(1):1-15.

Wu SW, Delgado MR, Maloney LT. 2015. Gambling on visual performance: neural correlates of metacognitive choice between visual lotteries. *Front Neurosci*. 9: 314.

Ye Q, Zou F, Dayan M, Lau H, Hu Y, Kwok SC. 2019. Individual susceptibility to TMS affirms the precuneal role in meta-memory upon recollection. *Brain Struct Funct*. 224(7): 2407-2419.

Ye Q, Zou F, Lau H, Hu Y, Kwok SC. 2018. Causal evidence for mnemonic metacognition in human precuneus. *J Neurosci*, 38(28): 6379-6387.

Yeatman JD, Dougherty RF, Myall NJ, Wandell BA, Feldman HM. 2012. Tract Profiles of White Matter Properties: Automating Fiber-Tract Quantification. *PLoS One*. 7(11): e49790.

Yeatman JD, Wandell BA, Mezer AA. 2014. Lifespan maturation and degeneration of human brain white matter. *Nat Commun*. 5(1):1-12.

Yeung N, Summerfield C. 2012. Metacognition in human decision-making: confidence and error monitoring. *Philos Trans R Soc Lond B Biol Sci*. 367(1594): 1310-1321.

Zeidman P, Mullally SL, Maguire EA. 2015. Constructing, perceiving, and maintaining scenes: Hippocampal activity and connectivity. *Cereb Cortex*. 25:3836–3855.

Zylberberg A, Fetsch CR, Shadlen MN. 2016. The influence of evidence volatility on choice, reaction time and confidence in a perceptual decision. *Elife*. 5: e17688.

Supplementary Materials:

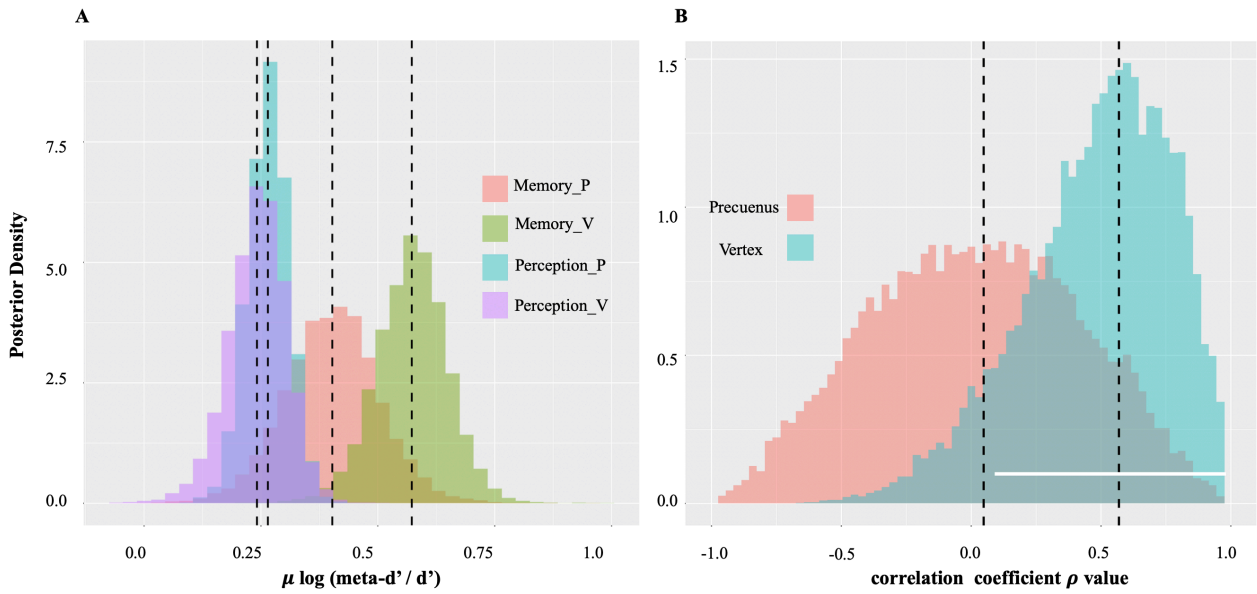

Figure S1. Behavioural metacognitive performance. ***A.*** Group posterior densities of metacognitive efficiency (log [meta-d' / d']) in perceptual and memory tasks in both TMS – precuneus and vertex conditions. The letter "P" in the legend represents TMS – precuneus condition, while "V" represents TMS – vertex condition. ***B.*** Posterior densities of the correlation coefficient ρ between metacognitive efficiencies in perceptual and mnemonic domains in both TMS – precuneus and vertex conditions. The white bar indicates the 95% Highest Density Interval (HDI) which excludes zero, indicating the correlation between perceptual and mnemonic metacognitive efficiency is significantly positive. The dotted lines in both figures show the ground-truth parameter values.

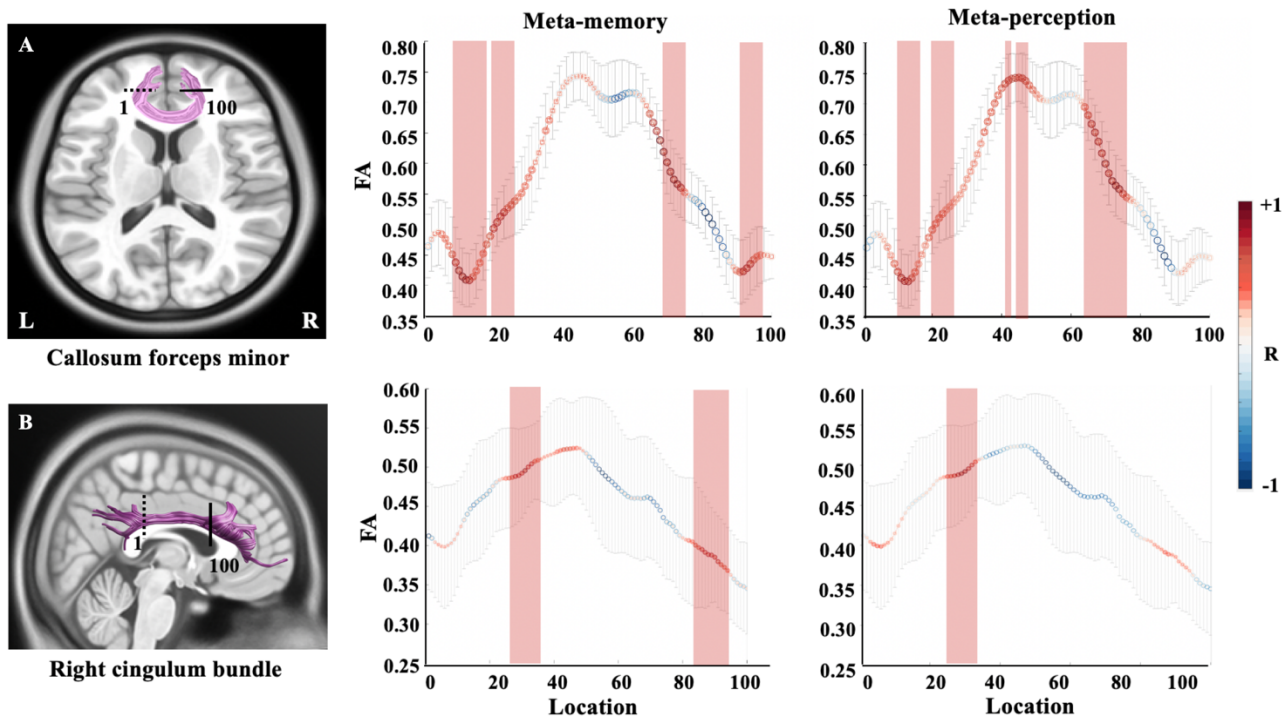

Figure S2. DTI results on callosum forceps minor (CFM) and right cingulum bundle (CB). The AFQ method divided the CFM and CB into 100 nodes. In the left panel, the dash line represents the location of the starting point (1) and the solid line represents the location of the ending point (100). The two panels on the right depict the correlations between the FA of a specific node and the metacognitive scores. ***A.*** The correlations of the CFM FA with mnemonic and perceptual metacognitive efficiency. ***B.*** The correlations of the right CB FA with mnemonic and perceptual metacognitive efficiency. The x-axis is the individual node alongside the SLF, and its corresponding FA value is shown on y-axis. The colour of the curved lines illustrates the correlation between the FA of a SLF node and metacognitive efficiency scores. Those nodes that had significant correlation with metacognitive efficiency scores are marked by a red rectangular (at an uncorrected threshold). The error bars denote standard error of the means over participants. Notes: DTI, diffusion tensor imaging; FA, fractional anisotropy; AFQ, Automating Fiber-Tract Quantification; CFM, callosum forceps minor; CB: cingulum bundle.